RESEARCH PAPER

Lung Disease Classification And Infection Region Detection Using MDCGRURNN Classifier

Dr. Nitha V R[1], Dr. Smitha John[2], Alphonsa Sini P J[3], Dr. Suja C Nair[4], Dr. Rasmi P S[5], Sneha Raj[6], Nikitha V[7], Tiny Thampan[8], Lintu Sara Jose[9], Rinu Treesa Philip[10], Annmary Sunny[11]

[1,6,7,8,9,11]CVV Institute of Science and Technology, Chinmaya Vishwa Vidyapeeth University, Ernakulam, India.

[2]Division of Information Technology, Cochin University of Science and Technology, Ernakulam, India.

[3]Department of Computer Science, Bhart Mata College, Thrikkakara, India.

[4]Associate Professor, CSE Department, Muthoot Institute of Technology and Science, Ernakulam

[5]Department of IT, Professor, Toc H Institute of Science & Technology, Ernakulam, India.

[10]Department of Computer Science, Assumption College, Changanassery, India.

Author for correspondence:

Dr. Nitha V R

CVV Institute of Science and Technology, Chinmaya Vishwa Vidyapeeth, Ernakulam, India., Email: nitha.vr@cvv.ac.in

ABSTRACT

One of the most prevalent respiratory conditions is pulmonary disease, and an accurate diagnosis is necessary to increase patient treatment efficacy. In the existing techniques, the infection region detected image contains occlusion and unwanted regions, which affect the severity analysis. In order to tackle these problems, the study proposed a lung disease infection region extraction and severity analysis using the SB DBDN classifier. The raw lung image data is first pre-processed, and the lung region is segmented using Distribution Median Heterogeneous Compound Symmetry Model-based Clustering (DMHCSMBC). The lung-affected regions are extracted using Max Intensity thresholding-based Pair-wise Region Comparison Predicate Graph-Based Segmentation (MITPRCPGBS). At the same time, the severity score is calculated for the lung segmented image and the detected image by using Fisher Block Matrices Scoring. Afterwards, the features are extracted from the infected region and patient metadata, followed by feature fusion and normalisation. Finally, the normalised features and severity scores are given to the Swish Bessel – Deep Belief Dense Network (SB-DBDN) to classify the severity. The outcome from the experiment illustrates that the SB-DBDN outperforms well.

Keywords: Distribution Median Heterogeneous Compound Symmetry Model-based Clustering, Max Intensity thresholding based Pair-wise Region Comparison Predicate Graph-Based Segmentation, Fisher Block Matrices Scoring, Swish Bessel – Deep Belief Dense Network, Deep learning.

How to cite this article: Nitha V R, Smitha John, Alphonsa Sini P J, Suja C Nair, Rasmi P S, Sneha Raj, Nikitha V, Tiny Thampan, Lintu Sara Jose, Rinu Treesa Philip, Annmary Sunny. Lung Disease Classification And Infection Region Detection Using MDCGRURNN Classifier. Int J Drug Deliv Technol. 2026;16(37s): 843-850. DOI: 10.25258/ijddt.16.37s.109

INTRODUCTION

Lung disease is a diverse collection of illnesses marked by lung parenchymal fibrosis in addition to inflammation [1, 2]. Many suffer from lung disease [3], and the world health organization reports that a considerable portion of deaths are triggered globally by respiratory illnesses, which include lung cancer, pneumonia, TB, asthma, chronic pulmonary obstruction, and lower respiratory tract infection [4]. It is mainly caused by smoking and pollution [5]. The majority of pulmonary cancer sufferers are still men. However, the number of afflicted women in their 30s and 40s is rising significantly [6]. Moreover, it can be totally cured using early detection [7]. Controlling the rising illness and mortality rate of lung disease requires early diagnosis and prompt treatment [8]. Additionally, there is a larger need to create an effective algorithm to identify lung disease[9].

It takes a while for a radiologist to analyse an individual's CT scans since it is challenging to categorise pulmonary abnormalities. Computer-aided diagnosis technologies have been designed to expedite the process [10, 11]. In the future, the CAD is enhanced with the new advancement in identifying severity. Examining the size measures and anomalies in the shape of the lungs, it offers information regarding the severity of lung illness [12]. Recent advances in the classification of the extent of the disease have mostly concentrated on particular deep learning features [13]. The subset of machine learning called deep learning has garnered a lot

of interest because of outstanding forecasting and categorizing performance [14]. Numerous machine learning algorithms are currently in use [15]. These types of algorithms are used to assist patients and doctors by identifying and assessing the efficacy of different deep learning algorithms related to lung ailments[16].

Related Works

Shakeel et al. [17] created an assessment of pulmonary scans to predict various abnormalities using the deep learning techniques that immediately train the neural networks and improve profuse clustering techniques. By using weighted mean histogram equalisation methods, the noise in the image was removed. The experiment showed results of higher accuracy with a minimum classification error. However, the suggested classifier was not apt while the large amount of data was used.

Huang et al. [18] introduced a novel deep convolutional neural network architecture to accomplish the interstitial lung disease pattern classification challenge. Additionally, to handle the issue of insufficient data for training, a unique learning of a two-stage transfer approach was introduced. This method used the data obtained from sufficient textural source information and additional unlabelled lung CT data in the target domain.

Guo et al. [19] proposed a small kernel DenseNet, an enhanced DenseNet, to enhance the performance of interstitial lung disease classification. The network proved more successful in extracting features based on the characteristics of computed tomography of lung disease. When feature patterns were minimal, the recognition efficiency was increased by using a small convolution kernel. The SK-DenseNet fared better than other CNNs, according to experiment data. However, the suggested network provided misclassification due to overfitting.

Asuntha et al. [20] showed a new technique for classifying lung cancer and its severity from an input lung image. The authors used the fuzzy particle swarm optimisation technique to choose the significant features. Ultimately, a unique FPSOCNN that lowered CNN's computing expenses was used to classify these features. The results of the experiment demonstrated that the new FPSOCNN excelled over other alternative methods. However, the FPSO technique suffered from early convergence in the primary stages.

MATERIALS AND METHODS

An FBMS-SB-DBDN methodology is suggested in identifying the severity of lung disease based on patient metadata. This proposed system contains two main phases. One is disease detection and another one is severity analysis. The block diagram of the proposing model is explained in Figure 1.

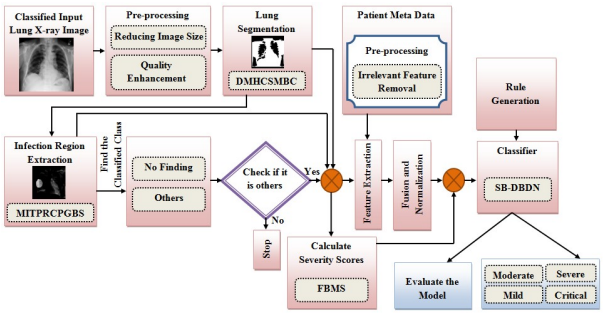

Pre-processing

In the proposed severity identifying system, NIH chest x-ray data [21] was used as the input to the proposed system. Due to the heterogeneity of the databases and as a result of variation in the sizes of images, the input images are resized, and the clarity of the images has been enhanced. This process yields an improved image that is better suited for the particular use than the original image, which is stated as,

$$R_n^{en} = \{R_1^{en}, R_2^{en}, ...R_n^{en}\} \quad [1]$$

where R_n^{en} represents the number of quality enhanced images.

Lung Segmentation

Following pre-processing, the x-ray image is segmented R_n^{en} using the distribution median heterogeneous compound symmetry model-based clustering. Model-based clustering is a statistical approach to data clustering. It involves dividing data on the probability of how a dataset belongs to a probability distribution, where each group represents different clusters. Even though the existing methods work efficiently, median heterogeneous compound symmetry method is introduced to get more accuracy in segmenting the infected region.

Each cluster k with the objects is modelled by the Gaussian distribution. Here, each point $o \in R_n^{en}$ is randomly assigned to one cluster ς_i.

The algorithm of the proposed DMHCSMBC is shown below as **Algorithm 1**.

Algorithm 1 Algorithm of the DMHCSMBC

Begin

Initialize parameters $o \in R_n^{en}$, M, d, ς_n
Compute probability density $\gamma_{den}(\mu_c, \Sigma_c)^{(o)}$
Calculate mean μ_ς and Hetrogeneous CS Σ_c
Compute combined density γ_{den}^{com}
Evaluate probability $\psi(\varsigma \mid o)$
Calculate log-likelihood χ
If (χ is high)
{
Data point corresponds to mixture
}
Else
{
Parameters are maximized
}
End if

Return L_n
End

Infection Affected Region Extraction

Following the lung segmentation, the affected regions are extracted from L_n using max intensity thresholding based on pairwise region comparison and predicate graph-based segmentation. A graph-based approach is the pairwise region comparison predicate. It defines the boundary between the regions and clusters the pixels based on the optimum thresholding. Although the graph-based segmentation model is more effective, the existing pair-wise method may segment the image with unwanted parts. In order to beat this issue, the proposed paper uses the max intensity thresholding for selecting the threshold level, which helps the system segment the interest region.

The existence of separation between two components in segmentation is based on a predicate. To evaluate the boundary between two components, the minimum inter-subgraph difference ($min\ C_{L_n}^{int}$) and the within-subgraph difference $\lambda_{L_n}^{diff}$ are calculated as,

$$min\ C_{L_n}^{int} = min(\ C_{aff}^{int} + \Delta(C_{aff}\ ), C_{non}^{int} + \Delta(C_{non})) \quad [2]$$

$$\lambda_n^{diff} = \min_{P_i \in C_{aff}, P_j \in C_{non}} \omega(P_{i,} P_j\ ) \quad [3]$$

Where, C_{aff} and C_{non} are the two different components, $\omega(P_i,P_j)$ weights of edges of the difference between two components, $\Delta(C_{aff})$ and $\Delta(C_{non})$ denote the threshold function of two components. The thresholding function controls the degree to which the within-subgraph difference must be greater than their inter-subgraph difference for there to be evidence of a boundary between them.

Where (i,j) represents the pixel coordinates, L_n^m the maximum intensity value pixel. Higher (Δ) might lead to higher $minC_{L_n}^{int}$, weakening the evidence for the boundary between components. When the threshold is higher, the boundary between inhomogeneous sub-regions that contain a similar texture is weakened. Hence, the unwanted regions are merged. When the threshold is low, the homogeneous region would strengthen its boundary. So the region can be merged accurately. In this way, the probability of inhomogeneous region emergence is decreased. By obtaining the difference, the pair-wise comparison predicate for evaluating the boundary of two components can be attained.

From this process, the output of the infected region λ_{Ln} can be obtained, and the detected image is classified as either the no finding class or another class. Afterwards, the condition is checked to identify whether the detected image has no findings or others. If it is others, then feature extraction is carried out.

Patient Metadata

Patient identity metadata Λ is nothing but medical records that comprise the attributes of patients. It includes the various features of the patient's name, age, sex, address, etc. From these, the irrelevant features, i.e. redundant features, are removed. After removing the redundant features, the pre-processed output Λ_{pre} can be obtained as,

$$\Lambda_{pre} = \eta_{eli}(\Lambda) \quad [4]$$

Where η_{eli} denotes the redundant elimination function.

Feature extraction

Features are collected from L_n ,$L1_n$ *and* Λ_{pre}. Here, the lower-level pixels are modified into higher-level representations, which help to gather useful information. Hence, the prominent features, such as visual, texture, intensity, and geometric moment features, are extracted from L_n and expressed as,

$$F_{L_n}^m = \{F_{L_n}^1, F_{L_n}^2, F_{L_n}^3, F_{L_n}^4\} \quad [5]$$

Where $F_{L_n}^m$ denotes the number of extracted features, is the number of features.

Visual feature: In this step, the histogram of oriented gradients was utilized to extract the visual features $F_{L_n}^1$. Initially, the gradient of the lung region for each pixel has been calculated. Based on the gradient, the magnitude and direction for each block are computed. Then, each block is normalised to reduce overbrightness, which leads to some parts of the image vanishing. To reduce

that, normalisation is used in particular parts, which is expressed as,

$$F_{L_n}^1 = \frac{\upsilon_{L_n}}{\|\upsilon_{L_n}\| + \circ} \quad (6)$$

Where ◦ represents a constant value, υ_{Ln} denote non-normalized vector. Finally, collecting normalised feature vectors represented in every horizontal and vertical block.

Texture feature: The statistical technique for extracting texture features is called the grey level co-occurrence matrix $F_{L_n}^2$ by analyzing the spatial correlation properties of grey scales in the lung-affected region. Texture features are defined over a lung image based on the distribution of co-occurring pixel values in the spatial position. The cooccurrence pixels have been added and represented in the form of a single pixel in the image. The single pixels are considered as the extracted features. It can be expressed as,

$$F_{L_n}^2 = F_{L_{n(con)}}^2, F_{L_{n(ent)}}^2, F_{L_{n(cor)}}^2 \quad (7)$$

Where, $F_{L_{n(con)}}^2$, $F_{L_{n(ent)}}^2$ and $F_{L_{n(cor)}}^2$ represent the contrast, entropy, and correlation of the lung affected region, respectively.

Intensity feature: In this feature extraction, the colors of the lung affected region are separated into a set of bins. Each bin is considered the same color space and stored. Then the intensity feature is expressed as,

$$F_{L_n}^3 = L_n(int)|L_n \quad (8)$$

Where $L_n(int)$ denotes the intensity of pixels, $F_{L_n}^3$ and denote the intensity feature.

Geometric moment features: The shapes of the image are used to extract the geometric moment features $F_{L_n}^4$. The kernel function is defined as a product of the pixel coordinates, making it the most basic moment function. It can be expressed as,

$$F_{L_n}^4 = \sum_{y=1}^{p} \sum_{x=1}^{Q} x_r y_s L_n(x.y) \quad (9)$$

Where r and s denote the kernel function for defining pixel coordinate (x,y). $L_n^R(x.y)$ represents the input image with pixel coordinates.

In this way, the features of patient metadata and lung-infected images are extracted for proceeding further, and the outputs $E_{L_m}^m$ $P_{\Lambda_{pre}}^m$ can be obtained. The three feature sets are consolidated into a single feature set by concatenating all the features. The fusion of features improves the stability and reliability of the recognition system performance, and then the features are normalised within the range. The fused K and normalised K features are expressed as

$$K = \iota(F_{L_n}^m, E_{L_n}^m, P_{\Lambda_{pre}}^m) \quad (11)$$

$$K = \frac{K}{\| K \|}$$

Where ι denotes the fusion function, $\| K \|$ is the length of the vector.

Calculating Severity Scores

The severity scores are calculated from L_n and $L1_n$ using Fisher block matrices scoring while the features are extracted. The Fisher scoring algorithm is typically an iterative process, and the minimal statistics needed for each iteration are the same as those needed for the related covariance problem analysis. But the existing methods are still lagging in providing accurate scores. To solve this issue, the proposed paper uses block metrics instead of covariance. In Fisher scoring, the steps that do not increase the likelihood are rejected, dividing the step size by 2 iteratively. If the likelihood cannot be increased along the Fisher step direction, the step is attempted along the gradient. Based on that, the Fisher scoring algorithm update rule takes the following form, γ

$$\gamma = (L_n \& L1_n) + C^{-1}(L_n \& L1_n) * \exists \quad (12)$$

$$C = \begin{bmatrix} C_{xx} & C_{xy} \\ C_{yx} & C_{yy} \end{bmatrix} \quad (13)$$

Where, L_n & $L1_n$ is the parameters in I^{th} iteration, $\exists$ denotes the constant, C^{-1} signifies the block matrix.

Classifier

In this section, the lung severity is classified from K' and γ using a swish Bessel – deep belief dense network. The layers in this network serve as feature detectors. Using a type of Markov random field known as the restricted Boltzmann network, the DBN learning stages begin by greedily learning the feature layer by layer, one layer at a time. Each RBM model generates output vectors in sequence after performing a nonlinear transformation on its input features. Following this learning phase, a DBN can be trained to do categorization under supervision. However, it is still difficult for the current network to provide an accurate prediction. The suggested paper triggered the dense layer and swish Bessel activation function to lessen the issue. The architecture of SB-DBDN is shown in Figure 2.

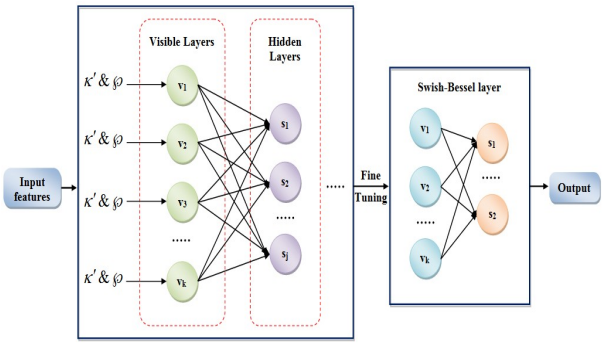

Fig. 2: structure of proposed SB-DBDN

Based on the score value calculated in the above step, rules are generated in addition to the inputs of K and γ. For example,

IF γ *is* ΦΦ *range THEN the output is* ∪ (14)

First, input features of severity scores and normalised features with the generated rules are given to the visible layer and dense layer, which compute the weighted average of its input, and it is expressed as,

$$D = W' * (K', \gamma) + B \quad (15)$$

Where w and B are randomly initialised weights and bias. Then the average weight is transferred into the hidden layers, and the energy function ε of the layer is calculated as,

$$\varepsilon = -\sum_{\Xi=1}^{\alpha}\sum_{\iota=1}^{\beta} D_{\Xi_\iota} v_\Xi s_\iota - \sum_{\Xi=1}^{\alpha} u_\Xi s_\Xi - \sum_{y=1}^{\beta} z_i s_i \quad (16)$$

Where $D_{\Xi\iota}$ represent weight values of the visible unit Ξ and hidden unit ι,α and β signify the number of the unit,u_Ξ and z_ι denote the bias in both layers, v_Ξ and s_ι denote stochastic visible and hidden variables. The process is continued till the last RBM layer. The output from hidden layers is given to the swish-bessel activation function, which takes in the output features from the previous cell and converts them into some form, and helps the network learn complex patterns in the data. The swish-bessel function ϕ_{swib} is calculated as,

$$\phi_{swib} = \varepsilon * \sigma(\varepsilon) \quad (17)$$

Where(ε) is the Bessel function, is expressed as,

$$\varepsilon^2 \frac{d^2t}{d\varepsilon^2} + \varepsilon \frac{dt}{d\varepsilon} + (\varepsilon - h)t = 0 \quad (18)$$

Where t denotes canonical solutions, h signifies an integer. In order this way, the data is tested, and the output can be obtained and categorized as mild, moderate, severe, and critical.

RESULTS & DISCUSSION

The proposed lung disease severity identification model is implemented using PYTHON 3.2.

Database Description

A subset of X-ray images from the publicly accessible NIH chest X-ray dataset was used in the proposed work to validate the performance. The 1,12,120 x-ray pictures with disease diagnoses from 30,805 distinct patients make up this NIH chest X-ray dataset. Eighty per cent of the data from the database is utilized for training, and twenty per cent is used for testing. Sample images of the dataset are shown in Figure 3.

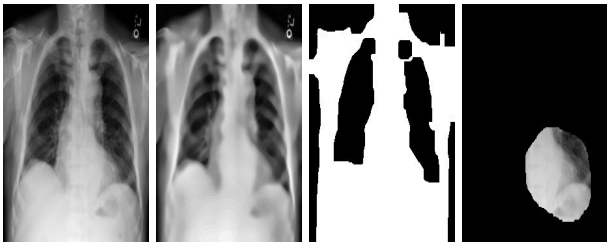

[a] [b] [c] [d]

Fig. 3: sample images with lung disease (a) input images, (b) contrast-enhanced image, (c) lung segmented image, (d) infected region segmented image

Performance analysis of classification

In this subsection, the performance of the proposed SB-DBDN method is analysed by comparing its outputs on various quality matrices with the existing deep belief network, residual neural network, AlexNetcnn, and convolution neural network methods.

Discussion: Figure 4 illustrates the SB-DBDN with existing methods based on the quality matrices. A higher value of the above metrics shows the higher performance of the proposed method. While analysing the performance of the proposed method, SBDBDN attains the accuracy of 98.89%, precision of 96.28%, recall of 99.22%, and sensitivity

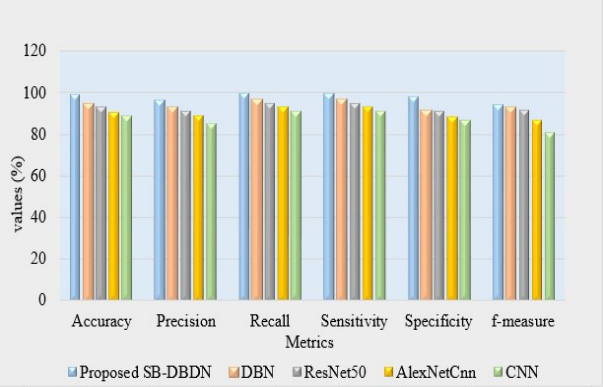

Fig. 4: Illustrates the performance of SB-DBDN with the existing methods

of 99.22%, specificity of 97.54%, and f-measure of 93.97%, which are higher than the existing methods. Higher performance is attained by a novel inducement of dense layer swish Bessel activation layer, which helps the system to learn the features accurately and produce the output within a short time. From the results, it can be summarised that the proposed SB-DBDN showed an efficient classification for the severity.

Table 1: Performance analysis of the proposed and existing methods

Techniques/Methods	**NPV**	**FPR**	**FNR**	**FRR**
Proposed SB-DBDN	95.5	3.3	0.41	0.41
DBN	91.9	45.6	0.88	0.88
ResNet50	91.1	49.2	38.2	38.2
AlexNetCnn	87.7	67.2	81.9	81.9
CNN	86.6	96.7	90.1	90.1

Discussion: Table 1 shows the analysis of the proposed SB-DBDN and existing models in terms of various quality matrices, and the higher value of negative predictive value and Matthews correlation coefficient shows the higher performance of the proposed method. The FNR and FRR of the proposed model are the same and show an improvement of 0.47% than DBN. Similarly, the improvement in FPR of the proposed method is 42.23% more than that of DBN. The NPV of the proposed methods showed an improvement by 3.55% than DBN. So, from the results of these metrics, it is concluded that the proposed SB-DBDN shows better performance for the classification of lung disease.

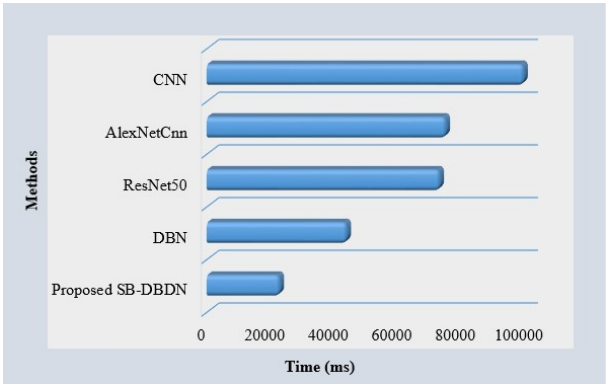

Fig. 5: Illustrates the computation time proposed with existing methods

Discussion: Figure 5 shows the amount of time needed for the suggested approach in comparison to the current approaches. When comparing the suggested method to DBN and other current approaches, it is evident that the latter have a laborious and complicated training process, whereas the suggested method uses swish-Bessel induction to carry out its process relatively quickly. Hence, the computational time of the proposed method is 22835ms, which is much lower when compared to the other existing methods of DBN (43874ms), ResNet50 (73054ms), AlexNetCnn(74986ms), and CNN(99384ms).

CONCLUSION

This paper proposes the SB-DBDN approach for the effective severity classification of lung disease as mild, moderate, severe, and critical. The proposed work involves seven stages, viz., pre-processing, lung segmentation, infection region extraction, feature extraction, calculating the severity score, fusion & normalisation, and classified severity analysis. In the experiment analysis, the suggested method is compared with state-of-the-art methods to evaluate the efficiency of the proposed SB-DBDN method. The performance of the suggested classifier is examined based on some quality metrics. Similarly, the computation time is analysed. In every stage of performance analysis, the experiment proved that the proposed methods attained a higher accuracy of 98.89% and a computation time of 22835ms. By focusing on the forecast of various stages at the minute level, the performance will be further enhanced in the future.

Declarations

There is no funding for this research. The authors declare that there is no competing interest and no ethical concern.

REFERENCE

[1] Shethwala, R., Pathar, S., Patel, T., Barot, P.: Transfer learning aided classification of lung sounds-wheezes and crackles. In: 2021 5th International Conference on Computing Methodologies and Communication (ICCMC), pp. 1260–1266 (2021). IEEE

[2] Wong, A.W., Ryerson, C.J., Guler, S.A.: Progression of fibrosing interstitial lung disease. Respiratory research 21(1), 32 (2020)

[3] Aykanat, M., Kılı¸c, O., Kurt, B., Saryal, S.B.: Lung disease classification using¨ machine learning algorithms. International Journal of Applied Mathematics Electronics and Computers 8(4), 125–132 (2020)

[4] Pham, L., Phan, H., Palaniappan, R., Mertins, A., McLoughlin, I.: Cnn-moe based framework for classification of respiratory anomalies and lung disease detection. IEEE journal of biomedical and health informatics 25(8), 2938–2947 (2021)

[5] Gupta, N., Gupta, D., Khanna, A., Rebou¸cas Filho, P.P., De Albuquerque, V.H.C.: Evolutionary algorithms for automatic lung disease detection. Measurement 140, 590–608 (2019)

[6] Ke, Q., Zhang, J., Wei, W., Pol ap, D., Wo´zniak, M., Ko´smider, L., Damaˇsevˇıs: A neuro-heuristic approach for recognition of lung diseases from x-ray images

[7] Gunasinghe, A.D., Aponso, A.C., Thirimanna, H.: Early prediction of lung diseases. In: 2019 IEEE 5th International Conference for Convergence in Technology (I2CT), pp. 1–4 (2019). IEEE

[8] Tariq, Z., Shah, S.K., Lee, Y.: Multimodal lung disease classification using deep convolutional neural network. In: 2020 IEEE International Conference on
Bioinformatics and Biomedicine (BIBM), pp. 2530–2537 (2020). IEEE

[9] Jayaraj, D., Sathiamoorthy, S.: Random forest based classification model for lung cancer prediction on computer tomography images. In: 2019 International Conference on Smart Systems and Inventive Technology (ICSSIT), pp. 100–104 (2019). IEEE

[10] Martinez, J.B., Gill, G.: Comparison of pre-trained vs domain-specific convolutional neural networks for classification of interstitial lung disease. In: 2019 International Conference on Computational Science and Computational Intelligence (CSCI), pp. 991–994 (2019). IEEE

[11] Monowar, K.F., Hasan, M.A.M., Shin, J.: Lung opacity classification with convolutional neural networks using chest x-rays. In: 2020 11th International Conference on Electrical and Computer Engineering (ICECE), pp. 169–172 (2020). IEEE

[12] Souza, J.C., Diniz, J.O.B., Ferreira, J.L., Da Silva, G.L.F., Silva, A.C., De Paiva, A.C.: An automatic method for lung segmentation and reconstruction in chest xray using deep neural networks. Computer methods and programs in biomedicine 177, 285–296 (2019)

[13] Baltruschat, I.M., Steinmeister, L., Ittrich, H., Adam, G., Nickisch, H., Saalbach, A., Berg, J., Grass, M., Knopp, T.: When does bone suppression and lung field segmentation improve chest x-ray disease classification? In: 2019 IEEE 16th International Symposium on Biomedical Imaging (ISBI 2019), pp. 1362–1366 (2019). IEEE

[14] Tariq, Z., Shah, S.K., Lee, Y.: Lung disease classification using deep convolutional neural network. In: 2019 IEEE International Conference on Bioinformatics and Biomedicine (BIBM), pp. 732–735 (2019). IEEE

[15] Radhika, P., Nair, R.A., Veena, G.: A comparative study of lung cancer detection using machine learning algorithms. In: 2019 IEEE International Conference on Electrical, Computer and Communication Technologies (ICECCT), pp. 1–4 (2019). IEEE

[16] Kavethanjali, V., Preethi, S., Vasanthapriya, V., et al.: Lung–pleura carcinoma detection using machine learning. In: 2021 3rd International Conference on Signal Processing and Communication (ICPSC), pp. 294–298 (2021). IEEE

[17] Shakeel, P.M., Burhanuddin, M.A., Desa, M.I.: Lung cancer detection from ct image using improved profuse clustering and deep learning instantaneously trained neural networks. Measurement 145, 702–712 (2019)

[18] Huang, S., Lee, F., Miao, R., Si, Q., Lu, C., Chen, Q.: A deep convolutional neural network architecture for interstitial lung disease pattern classification. Medical & biological engineering & computing 58(4), 725–737 (2020)

[19] Guo, W., Xu, Z., Zhang, H.: Interstitial lung disease classification using improved densenet. Multimedia Tools and Applications 78(21), 30615–30626 (2019)

[20] Asuntha, A., Srinivasan, A.: Deep learning for lung cancer detection and classification. Multimedia Tools and Applications 79(11), 7731–7762 (2020)

[21] Wang, X., Peng, Y., Lu, L., Lu, Z., Bagheri, M., Summers, R.M.: Chestx-ray8: Hospital-scale chest x-ray database and benchmarks on weakly-supervised classification and localization of common thorax diseases. In: Proceedings of the IEEE Conference on Computer Vision and Pattern Recognition (CVPR), pp. 3462–3471 (2017). https://doi.org/10.1109/CVPR.2017.369